Optical absorption of $KTa_{1-x}Nb_xO_3$ single crystals

Y. Brada*
Racah Physics Institute, The Hebrew University of Jerusalem, Jerusalem 91904, Israel

M. Roth†
School of Applied Science, The Hebrew University of Jerusalem, Jerusalem 91904, Israel

(Received 4 October 1988)

The optical absorption at photon energies near the fundamental absorption edge was measured in the cubic phase of $KTa_{1-x}Nb_xO_3$ crystals, both in a "pure" sample and in an (Fe,Ti)-doped case. In the first case the absorption constant followed the exponential Urbach rule, with a single steep slope, while in the second case two distinct slopes of lower values were clearly discernible, each in its own separate energy range. The range of temperatures applied to the samples was between 77 and 373 K. The functional temperature dependence of the slopes indicates that in both cases strains and impurities have a predominant influence through their constant electrical fields. On the other hand, the temperature shift of the optical-gap energy has been ascertained in both cases as being due to an internal Franz-Keldysh effect of the electrical fields created by the 25-meV LO_1 phonons.

I. INTRODUCTION

In connection with the growing interest in the optical properties of $KTa_{1-x}Nb_xO_3$- (KTN-) type ferroelectric crystals as optoelectronic materials, we measured the fundamental absorption edge in two types of crystals, one of "pure" consistency and the other heavily doped by Fe and Ti. The influence of temperature on these properties is also of major interest. As the crystalline structure changes with temperature, the temperatures were chosen so that the particular crystals would be in the cubic configuration.

II. EXPERIMENTAL

The crystals were grown on seeds from solutions in molten potassium carbonate at constant temperature in order to obtain large homogeneous samples.[1] In the case of doping, the dopands were present in the melt. The doped crystals, even though they were single crystals, showed a gradient of concentration of the additives which was observable due to coloration changes along the growth direction.

After growth and annealing, the crystals were cut, polished, measured, photographed under a polarizing microscope, chemically characterized by an electron microprobe, and then mounted on a cold finger in a vacuum cryostat. A random distribution of localized strains was visible through their birefringence under the polarizing microscope. The crystals reported here are described in Table I. For electrical measurements, which will be reported later,[2] electrodes were applied by brush or evaporation.

The optical system consisted of stabilized light sources, a SPEX double monochromator with low stray light, and photomultipliers both for detection and referencing purposes. The whole system was computer controlled, as was the data collection and storage.

III. EXPERIMENTAL RESULTS

A. The slope of the absorption edge as a function of doping and temperature

Crystal 1 is the "pure" crystal, and measurement showed a prominent strong absorption edge with only a weak "tail" at lower energies, as was also observed in other not-completely-pure crystals.[3–5] This high-density absorption edge was measured at a number of stabilized temperatures between 77 and 373 K.

Figure 1 represents such an absorption curve at the given temperature. The measured absorption constants have an exponential character, in accordance with the Urbach rule:[6,7]

$$\alpha=\alpha_0\exp[S(E-E_0)] , \quad (1)$$

TABLE I. The physical properties of the reported crystals. The parameters are explained in the text. The accuracies of the parameters expressed in eV are ±1 meV.

Crystal	Dimensions (mm^3)	at. %	E_0 (eV)	$E(0)$ (eV)	$\hbar\omega$ (meV)	α_g (cm^{-1})
1	8.5×4.0×2.98	Ta, 95; Nb, 5	3.545	3.485	23±2	20.1
2	2.5×2.2×1.1	Ta, 94; Nb, 5 Ti, 0.53; Fe, 0.16	3.488	3.435	24±1	58.01

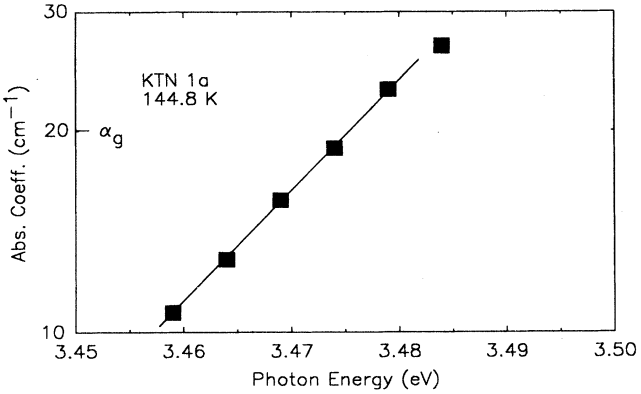

FIG. 1. The absorption constant of crystal 1 as a function of energy. The energy at absorption of $\alpha d=6$ was taken as the value proportional to E_g. α_g, the absorption coefficient there, is 20.1 cm^{-1}. The slope "S" in eV^{-1} was taken from these representations.

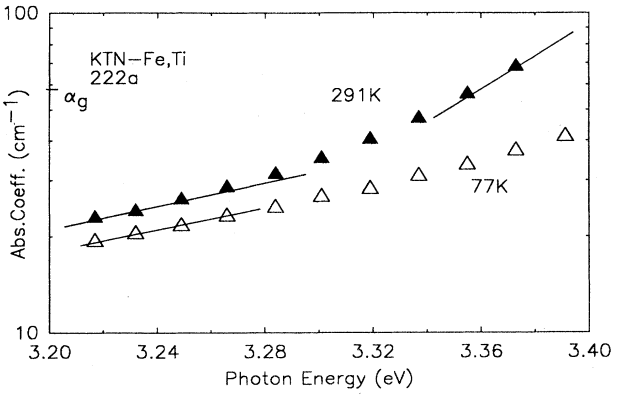

FIG. 3. The absorption constant of crystal 2 as a function of photon energies, measured at 77 and 291 K.

where α_0 and E_0 are constants, S is the measure of the slope (in eV^{-1}), and E is the photon energy. The theoretical relationships have been developed for the so-called slope parameter σ which is related to S through

$$\sigma = SkT \ , \tag{2}$$

where k and T have the usual meaning. Figure 2 represents the results for crystal 1 and shows the behavior of this slope parameter with temperature over the measured temperature range. A good approximation to a linear temperature dependence is observed. The interpretation of this fact will be given in the Discussion. The doped crystal, sample 2, was measured under the same circumstances. Figure 3 represents partial results at two temperatures. Two clearly discernible absorption slopes are documented in Fig. 3, the steeper slope belonging to the highest energy range measurable. Figure 4 sums up these experiments, and as can be seen from the data, both slopes again show a linear relationship with temperature. Nevertheless, the lower curve of Fig. 4 shows a gradual increase in the gradient of the slope parameter at the higher temperatures. The theoretical significance of these observations will be discussed later.

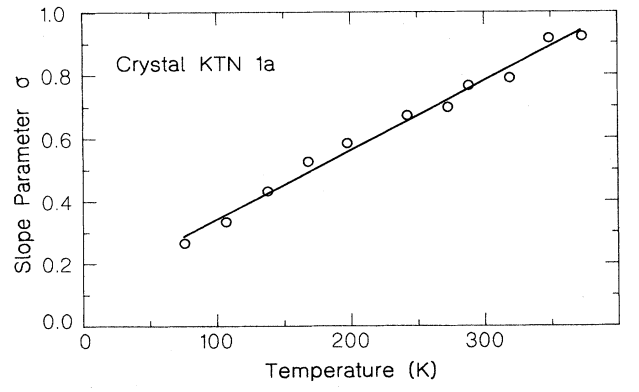

FIG. 2. The slope parameter of crystal 1 as a function of temperature. The slope parameter was taken as SkT.

B. The shift of the absorption-edge energy with temperature

The optical-absorption edges of most transparent materials shift with temperature changes. This is true also of the KTN crystals. In all cases the shift of the energy value of the photon at a constant and high value of α_g was measured; this is then proportional, with a constant of proportionality,[8] to the shift of E_g, the energy-gap value. Figure 5(a) gives a graphical representation of the results for crystal 1; the functional relationship will be explained later. Figure 5(b) shows the same data represented in another functional relationship. Figures 6(a) and 6(b) represent the data of the results as obtained for the doped crystal 2, again in the same functional representations.

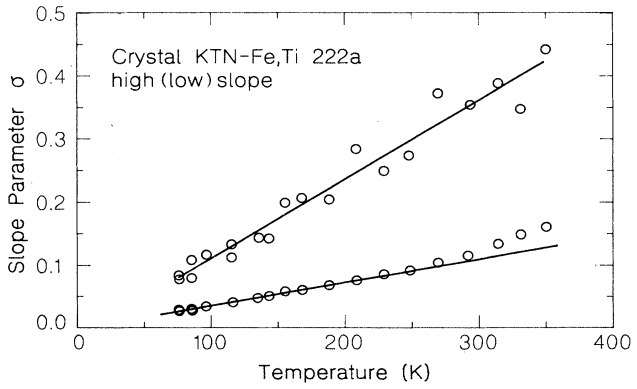

FIG. 4. The slope parameters of crystal 2. The average energy of the photon of the steeper slope was 3.39 eV; at the lower slope it was 3.25 eV. The increase of the lower slope at the higher temperatures is due to the gradual shift of the absorption edge to lower energies.

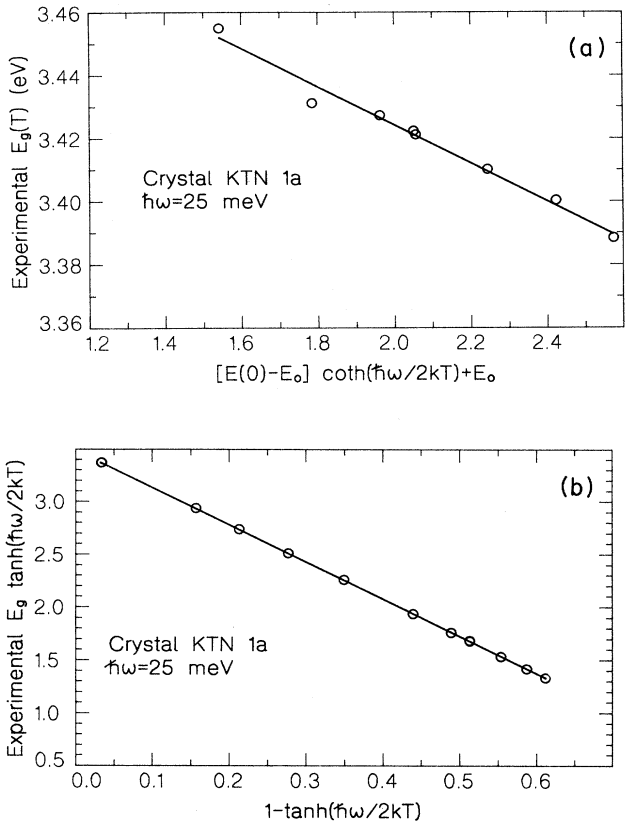

FIG. 5. (a) The shift of $\alpha_g = 20.1\ \text{cm}^{-1}$ as a function of temperature in crystal 1, represented with the help of Eq. (6a), and the phonon energy taken as 25 meV. (b) Same as (a), but with use of Eq. (6b).

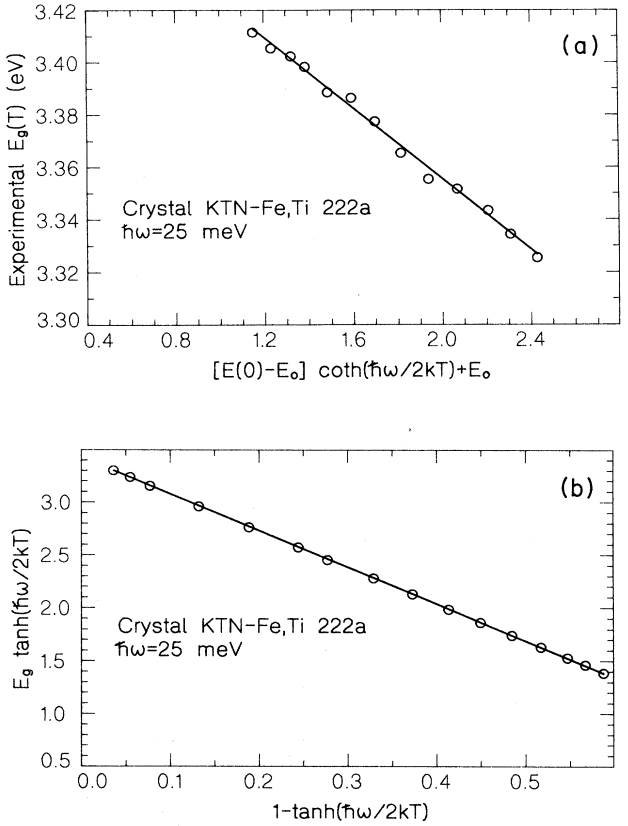

FIG. 6. (a) The shift with temperature of $\alpha_g = 58.01\ \text{cm}^{-1}$ in crystal represented with the help of Eq. (6a), and the phonon energy taken as 25 meV. (b) Same as (a), but with use of Eq. (6b).

IV. DISCUSSION

We will discuss our results on the basis of the Dow-Redfield theory.[9] In previous publications we discussed the influence of both external and internal, impurity- and phonon-generated electrical fields, on the optical properties of partly ionic solids having piezoelectric and longitudinal-optical phonons.[3–5,8,10] In contrast with indirect-gap materials, where the phonons contribute to the temperature shift of the absorption edge by supplying the needed change in momentum, we observe in direct-gap materials effects connected with the above-mentioned internal fields through an internal Franz-Keldysh effect. This was also found to be the reason for the Urbach tail in ionic crystals.[9,11–14] It has been shown that any other effects, such as thermal dilatation, have a much smaller influence on the previously reported optical measurements[15–17] in partly ionic crystals. Of course, this effect of internal, phonon-generated electrical fields has to be checked by comparing the functional dependences of the measured parameters with theory.

We will discuss the slope parameter first. The theoretical form for this parameter as computed for pure ionic crystals is[18–21]

$$\sigma = \sigma_0 \theta^{-1} \tanh(\theta) , \tag{3}$$

where

$$\theta = \hbar\omega/2kT . \tag{4}$$

Here σ_0 is a constant which is proportional to the reciprocal of the volume of the excited state (exciton) of the transition.[21] The expression $\hbar\omega$ represents the energy of the active phonon. It has also been shown that if the fields generated by the phonons are small (low-energy phonons) and the crystals are not chemically homogeneous, such as in mixed crystals and heavily doped crystals, the electrical internal fields due to these latter defects prevail and the phonon contribution is obscured.[10,14,23] In such cases σ will shift linearly with temperature, just as observed in both reported samples (Figs. 2 and 4). The prevalence of the constant strain-dislocation-, and impurity-generated electrical fields is then the necessary conclusion from these experiments.

The internal fields will also shift the absorption-edge energy through an Franz-Keldysh effect by enabling the partial tunneling of electrons through the forbidden region.[11,12] Using the results from our previous work[8,13] we can write the LO-phonon-induced field as

$$F_p(T) = F_p(0)\coth(\theta) , \tag{5}$$

where $F_p(0)$ is the field at $T=0$ and θ is given by Eq. (4).

Further computation brings us to the relationship

$$E_g(T)=E_g(0)\coth(\theta)-E_0[\coth(\theta)-1] , \quad (6)$$

where $E_g(T)$ is the gap energy at temperature T. After rearrangement Eq. (6) results in

$$E_g(T)=[E_g(0)-E_0]\coth(\theta)+E_0 . \quad (7)$$

A graphic representation can be made from this functional dependence, and then, using a least-squares approach, all the constants can be found. This approach is preferable to another variation on the solution which results in the mapping

$$E_g\tanh(\theta)=E_g(0)-E_0[1-\tanh(\theta)] , \quad (8)$$

as these functions are graphically less sensitive to variations of $\hbar\omega$. Both functions have been represented with $E_g(T)$ being the measured values of the gap energy, or, properly speaking, an energy proportional to the gap energy,[8] which has the same functional temperature dependence. From the good fit of the line to the experimentally obtained values, the numerical data can be computed. The results are represented in Table I. The used computational approach involves the least-squares method, with the phonon frequency being the adjustable parameter. The results from both graphical representations of course give very similar numerical values in both cases, as the equations are directly convertible.

The thermal shift of the absorption edge also explains the gradual increase of the gradient of the lower slope in Fig. 4, as the gap energy decreases and the constant-photon-energy points slowly enter the high-slope region, as can be seen from Fig. 3.

V. CONCLUSIONS

Both the form and the energy of the fundamental absorption edge of the partly ionic crystals of pure and strongly doped KTN show the predominant influence of internal electric fields. The slope is in both cases determined by the strain- and impurity-induced electrical fields and its slope parameter therefore shows a linear dependence on temperature. On the other hand, the thermal shift of the gap energy is clearly due to the 25-meV LO_1 phonons[22] via their electrical fields. This is documented by the functional dependence of this thermal-gap shift on the hyperbolic functions of the phonon energy and temperature.

*On leave of absence at Syracuse University, Department of Physics, 201 Physics Building, Syracuse, NY 13244-1130.
†On leave of absence at Marshall Air Center, NASA Code ES75, Huntsville, AL 35812.

[1]P. W. Whipps, J. Cryst. Growth **12**, 120 (1972).
[2]Y. Brada *et al.* (unpublished).
[3]B. G. Yacobi *et al.*, Phys. Rev. B **11**, 2990 (1975).
[4]Y. Brada *et al.*, Solid State Commun. **17**, 193 (1975).
[5]B. G. Yacobi and Y. Brada, Solid State Commun. **18**, 135 (1976).
[6]F. Urbach, Phys. Rev. **92**, 1324 (1953).
[7]W. Martienssen, J. Phys. Chem. Solids **2**, 257 (1957).
[8]L. Samuel *et al.*, Phys. Rev. B **36**, 1174 (1987).
[9]J. D. Dow and D. Redfield, Phys. Rev. B **5**, 594 (1972).
[10]L. Samuel *et al.*, Phys. Rev. B **37**, 4671 (1988).
[11]W. Franz, Z. Naturforsch. **13a**, 484 (1958).
[12]L. V. Keldysh, Zh. Eksp. Teor. Fiz. **34**, 1138 (1958) [Sov. Phys.—JETP **7**, 788 (1958)].
[13]L. Samuel *et al.*, Phys. Rev. B **36**, 1168 (1987).
[14]D. Redfield and M. A. Afromowitz, Appl. Phys. Lett. **11**, 138 (1967).
[15]F. Moglich *et al.*, Z. Techn. Phys. **21**, 6 (1940).
[16]H. Y. Fan, Phys. Rev. **82**, 900 (1951).
[17]W. W. Piper *et al.*, J. Phys. Chem. Solids **8**, 457 (1957).
[18]H. Mahr, Phys. Rev. **125**, 1510 (1962); **132**, 1880 (1963).
[19]M. V. Kurik, Phys. Status Solidi A **8**, 9 (1971).
[20]H. Migazaki and E. Hanamura, J. Phys. Soc. Jpn. **50**, 1310 (1980).
[21]Y. Toyozawa and M. Schreiber, J. Phys. Soc. Jpn. **51**, 1528 (1982).
[22]Y. Yacoby and A. Linz, Phys. Rev. B **9**, 2723 (1974).
[23]Qiming Li *et al.*, Phys. Rev. B **37**, 8289 (1988).